

Investigation of fundamental properties of the $\bar{K}NN$ state

2023/08/17. Yuto Kimura

1. Introduction

• E15

Quasi-free $K^-N \rightarrow \bar{K}n$ によって n が knock out

$\theta_n = 0, \pi$ に Quasi free の event が集中

~on-shell kaon の momentum
(= momentum transfer)

Mass threshold の下に sub structure

K^-pp ($\bar{K}NN$ for $I_z = +1/2$) の束縛状態を示唆

なるべく $q_{\Lambda p}$ が小さい方が束縛状態を作りやすい

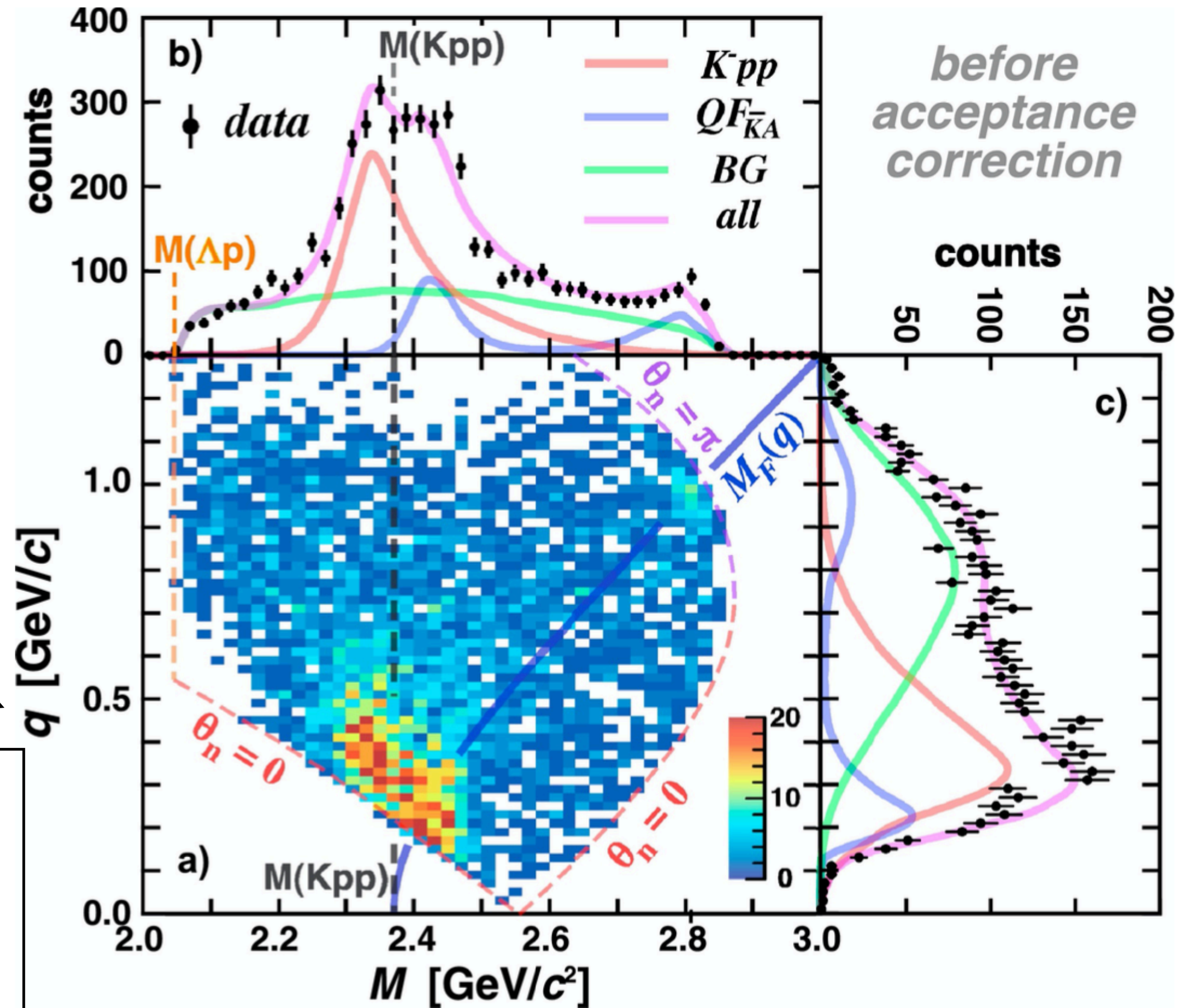
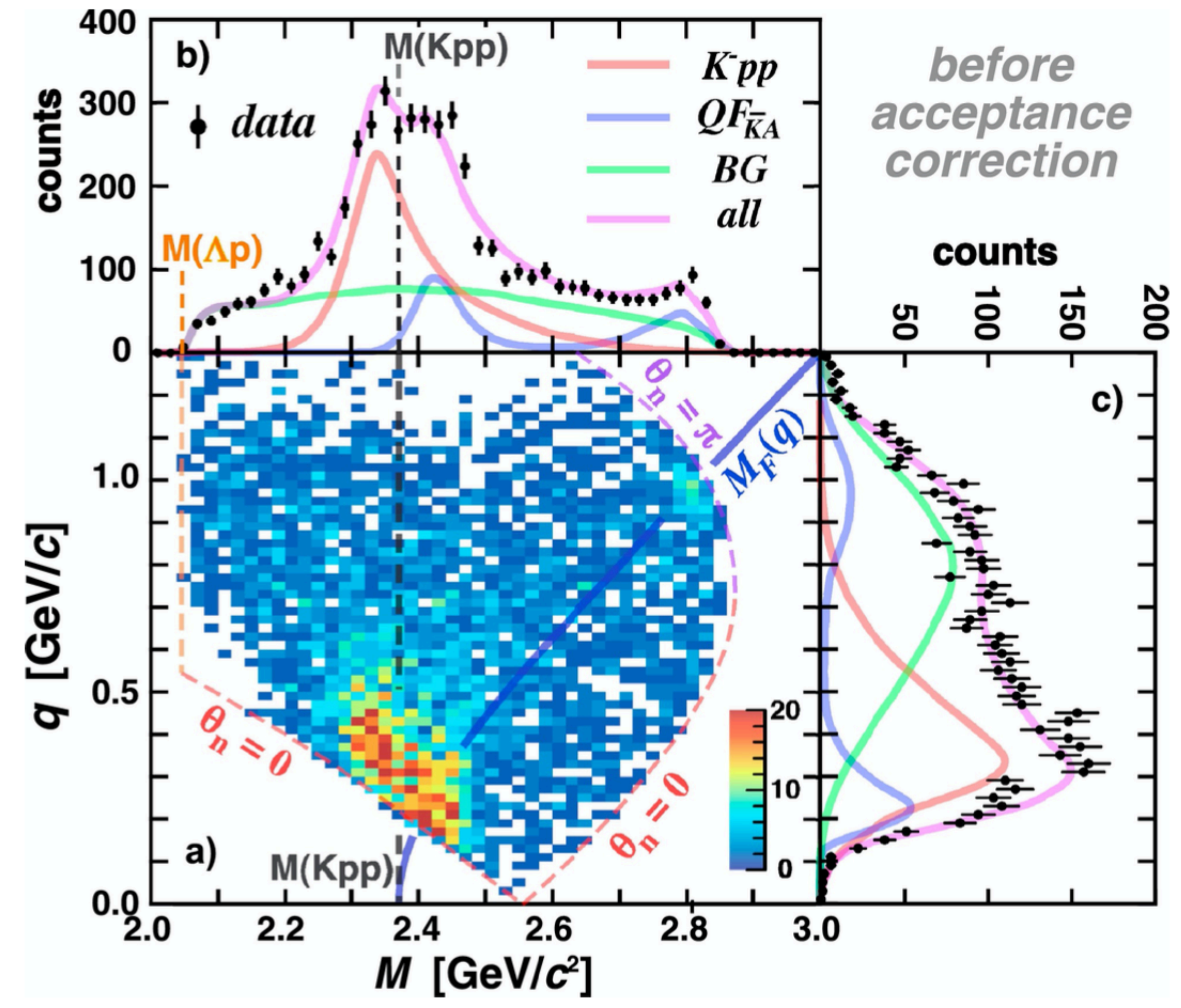
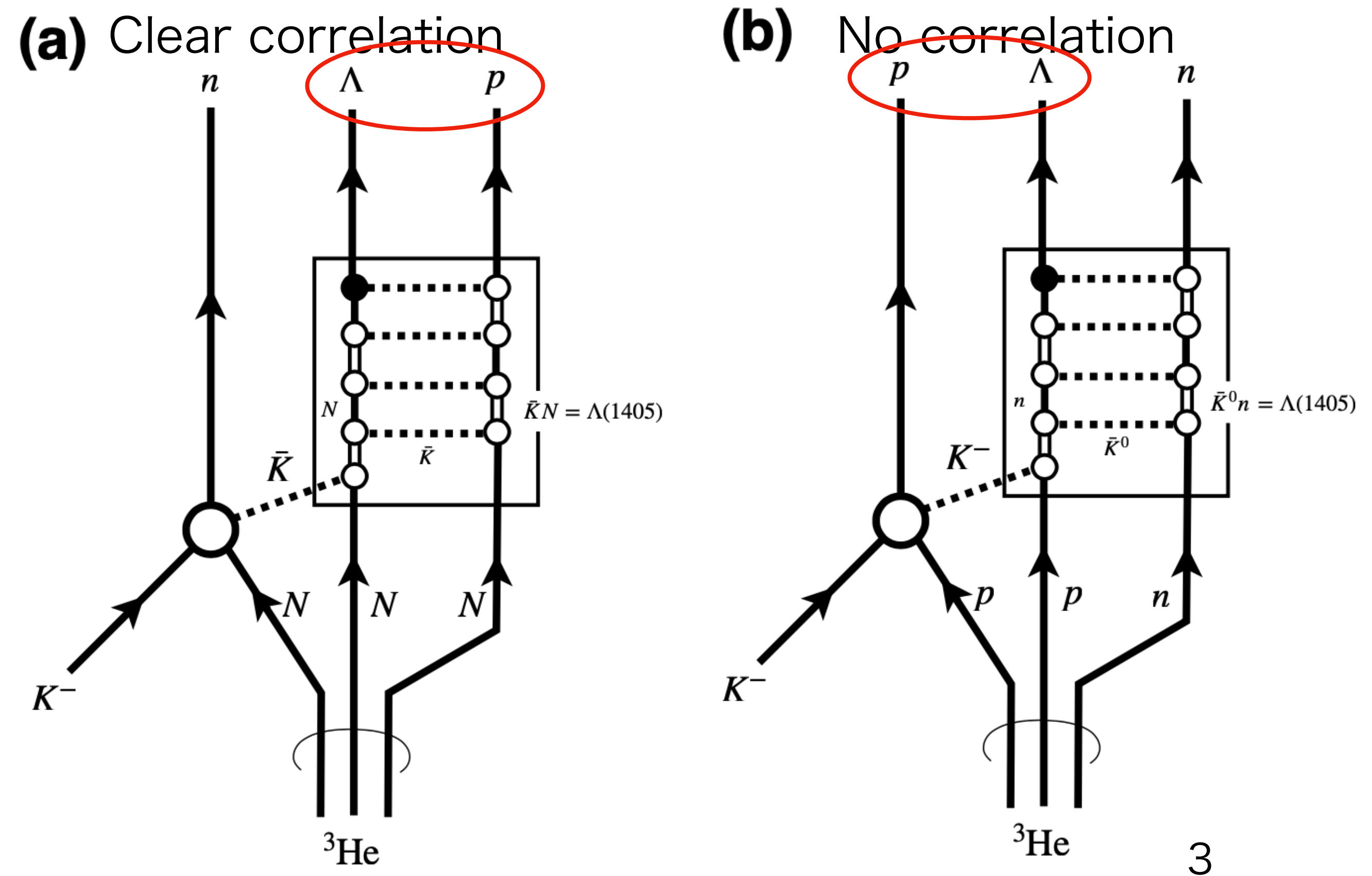


Figure 1: (a) Two dimensional event distribution on the plane of the Λp invariant-mass ($m_{\Lambda p}$) and momentum transfer to the Λp system ($q_{\Lambda p}$). (b) and (c) are spectral projections on $m_{\Lambda p}$ and $q_{\Lambda p}$ axes, respectively. The colored lines in (b) and (c) are the fitting result. The figure was taken from Ref. [20].

1. Intro

- E15
- BGについて

Broad distribution = no correlation
 Misconceiving analysis (b) 由来?



(a) Two dimensional event distribution on the plane of the Λp invariant mass ($M_{\Lambda p}$) and momentum transfer to the Λp system ($q_{\Lambda p}$). (b) and (c) are marginal plots on $m_{\Lambda p}$ and $q_{\Lambda p}$ axes, respectively. The colored lines in (b) and (c) are fits to the data. The figure was taken from Ref. [20].

1. Intro

- E15を超えて

• Λp 以外にもdecay channelがある →より詳細なcross section・branching ratio

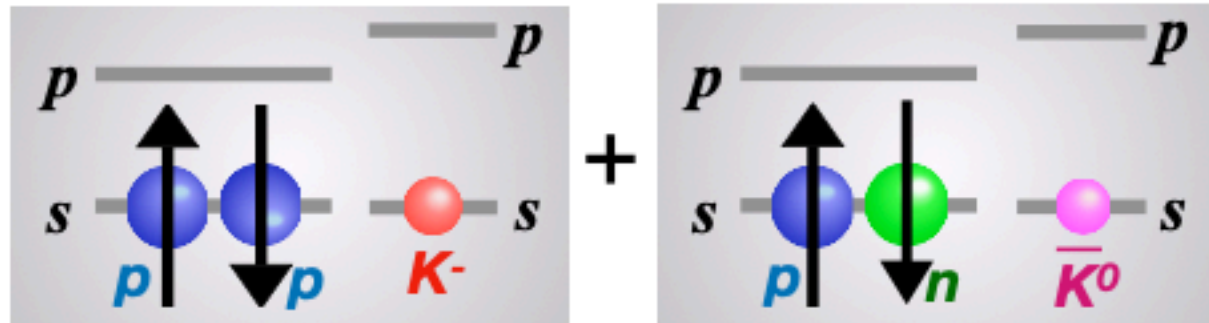
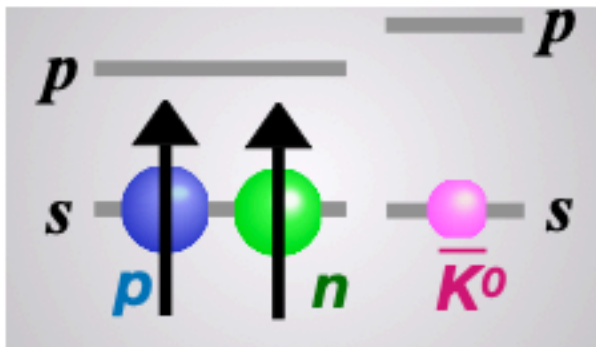
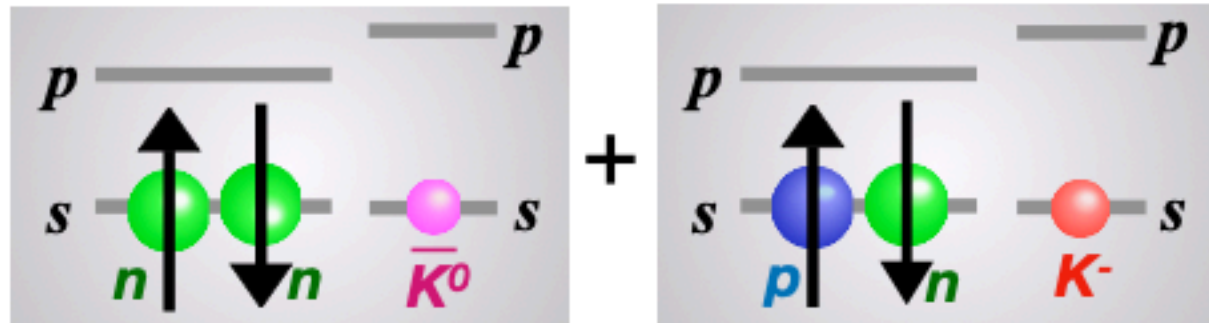
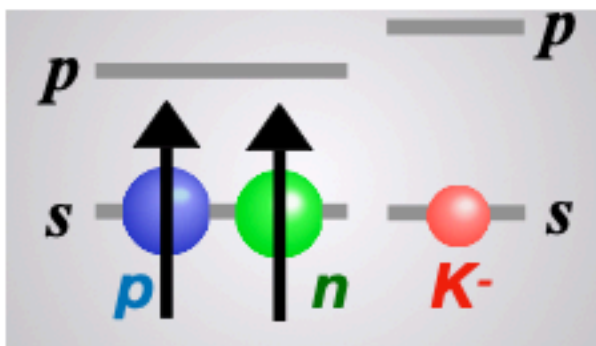
• $\bar{K}NN \rightarrow \Lambda N, \Sigma N$ のbranching ratioから $\Lambda(1405)$ の寄与も調べられる



The key to access these channel is the sufficient neutron detection capability.

2. Internal configuration and J^P of $\bar{K}NN$

Table 1: Internal configuration of $\bar{K}NN$ with $J^P = 0^-$ and 1^- .

$I (J^P)$	$\frac{1}{2} (0^-)$ Ground state の候補	$\frac{1}{2} (1^-)$
NN symmetry	$(NN)_{I.sym \times S.asym} \otimes \bar{K}$ $I_{NN} = 1, S_{NN} = 0$	$(NN)_{I.asym \times S.sym} \otimes \bar{K}$ $I_{NN} = 0, S_{NN} = 1$
$I_z = +\frac{1}{2}$	 $-\sqrt{\frac{1}{3}} \left(\sqrt{2} ppK^- + \frac{pn+np}{\sqrt{2}} \bar{K}^0 \right) \otimes \left(\frac{\uparrow\downarrow - \downarrow\uparrow}{\sqrt{2}} \right)$	 $\frac{(pn - np)}{\sqrt{2}} \bar{K}^0 \otimes \left(\uparrow\uparrow, \frac{\uparrow\downarrow + \downarrow\uparrow}{\sqrt{2}}, \downarrow\downarrow \right)$
$\bar{K}^0 nn$ も考えるべき $I_z = -\frac{1}{2}$	 $-\sqrt{\frac{1}{3}} \left(\sqrt{2} nn\bar{K}^0 + \frac{pn+np}{\sqrt{2}} K^- \right) \otimes \left(\frac{\uparrow\downarrow - \downarrow\uparrow}{\sqrt{2}} \right)$	 $-\frac{(pn - np)}{\sqrt{2}} K^- \otimes \left(\uparrow\uparrow, \frac{\uparrow\downarrow + \downarrow\uparrow}{\sqrt{2}}, \downarrow\downarrow \right)$
$\bar{K}N$ coupling	$\frac{ I_{\bar{K}N=0} ^2}{ I_{\bar{K}N=1} ^2} = \frac{3}{1}$	$\frac{ I_{\bar{K}N=0} ^2}{ I_{\bar{K}N=1} ^2} = \frac{1}{3}$

2. Internal configuration and J^P of $\bar{K}NN$

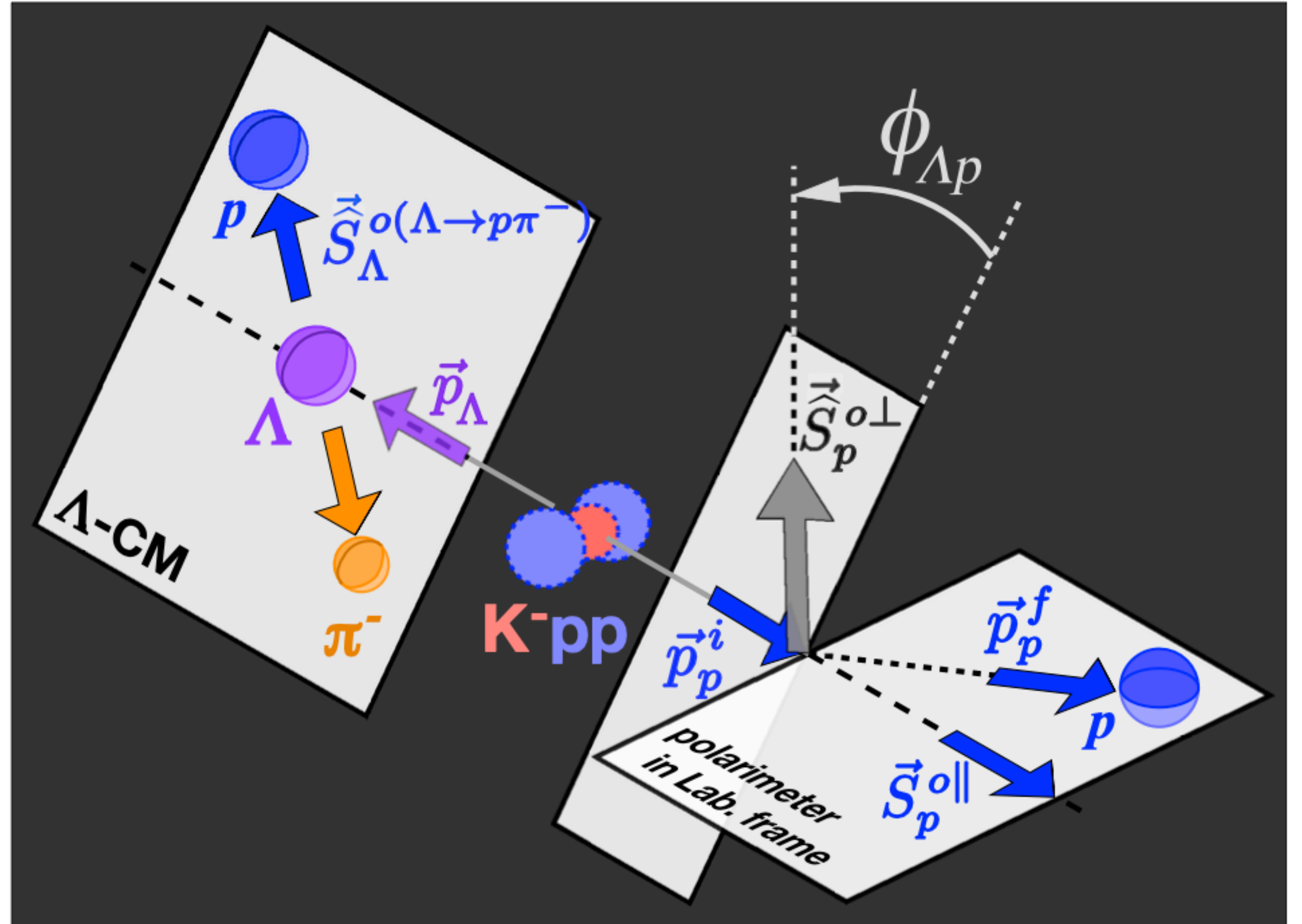
- $\bar{K}^0 pp, K^- nn$ は考えない。($\bar{K}N$ が $I = 1$ にしかないので)
- $I_{\bar{K}N} = 0$ がメインの $J^P = 0^-$ が ground stateであり、束縛される。
- $J^P = 1^-$ は束縛されないと予想されている。
- 実験的に J^P を決定することで $\bar{K}NN$ のより深い理解につながる。

3. Experimental method

$\bar{K}NN$ の J^P の決め方

- $\sigma_{\bar{K}^0nn}/\sigma_{K^-pp}$ を実験で求める。(間接的)
- $N(\phi_{\Lambda p}) = N_0 \left(1 + r^{JP} \cdot \alpha_{\Lambda p} \cos \phi_{\Lambda p} \right),$

から相関係数 α を求める。(直接的)



4. Experimental setup

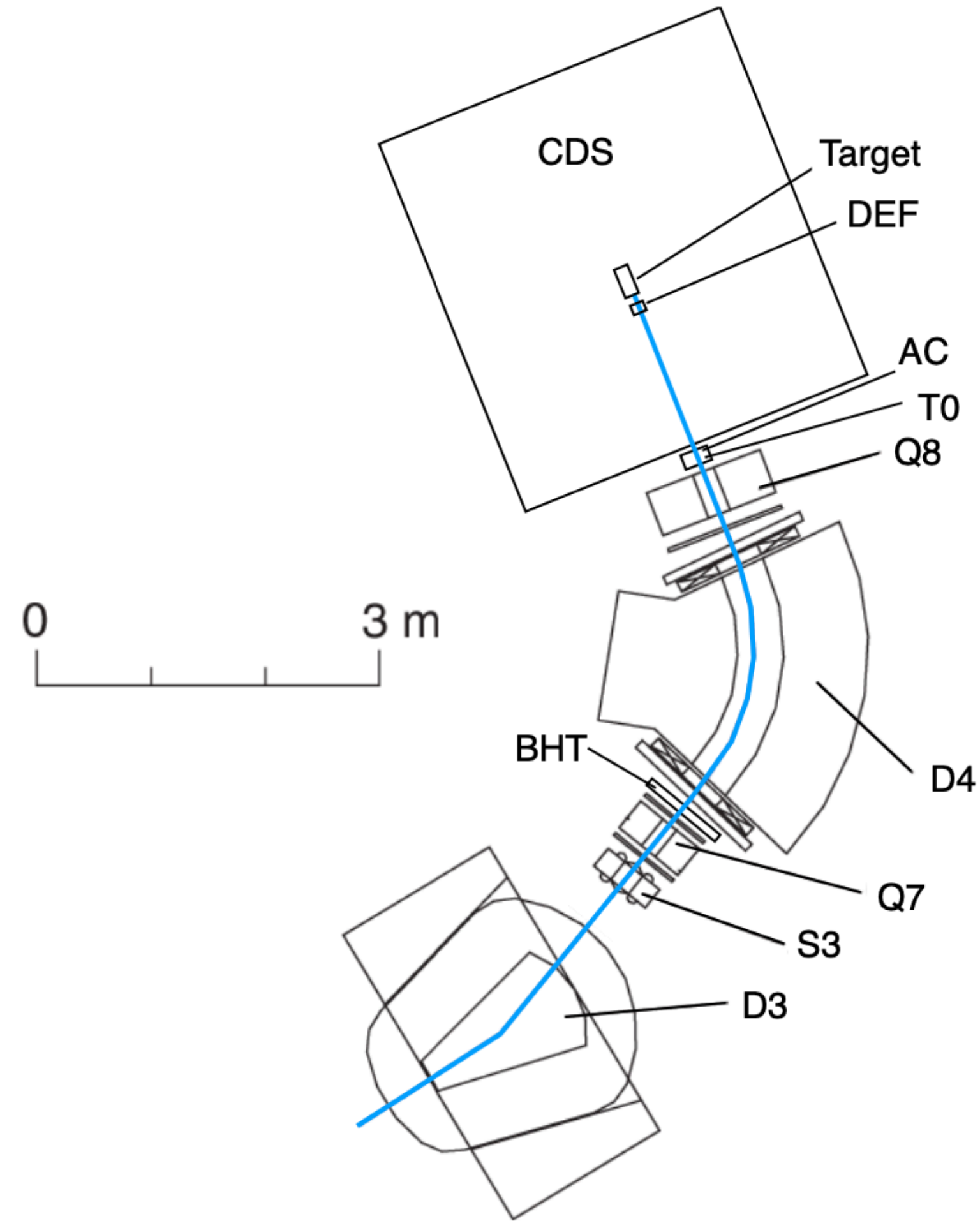


Figure 4: Schematic drawing of the K1.8BR beam-line with a shortened configuration of the beam-line proposed in E80 [29].

4. Experimental setup

Trigger
 $(\overline{\text{BHT}} \otimes \text{T0} \otimes \text{DEF} \otimes \overline{\text{AC}})$.

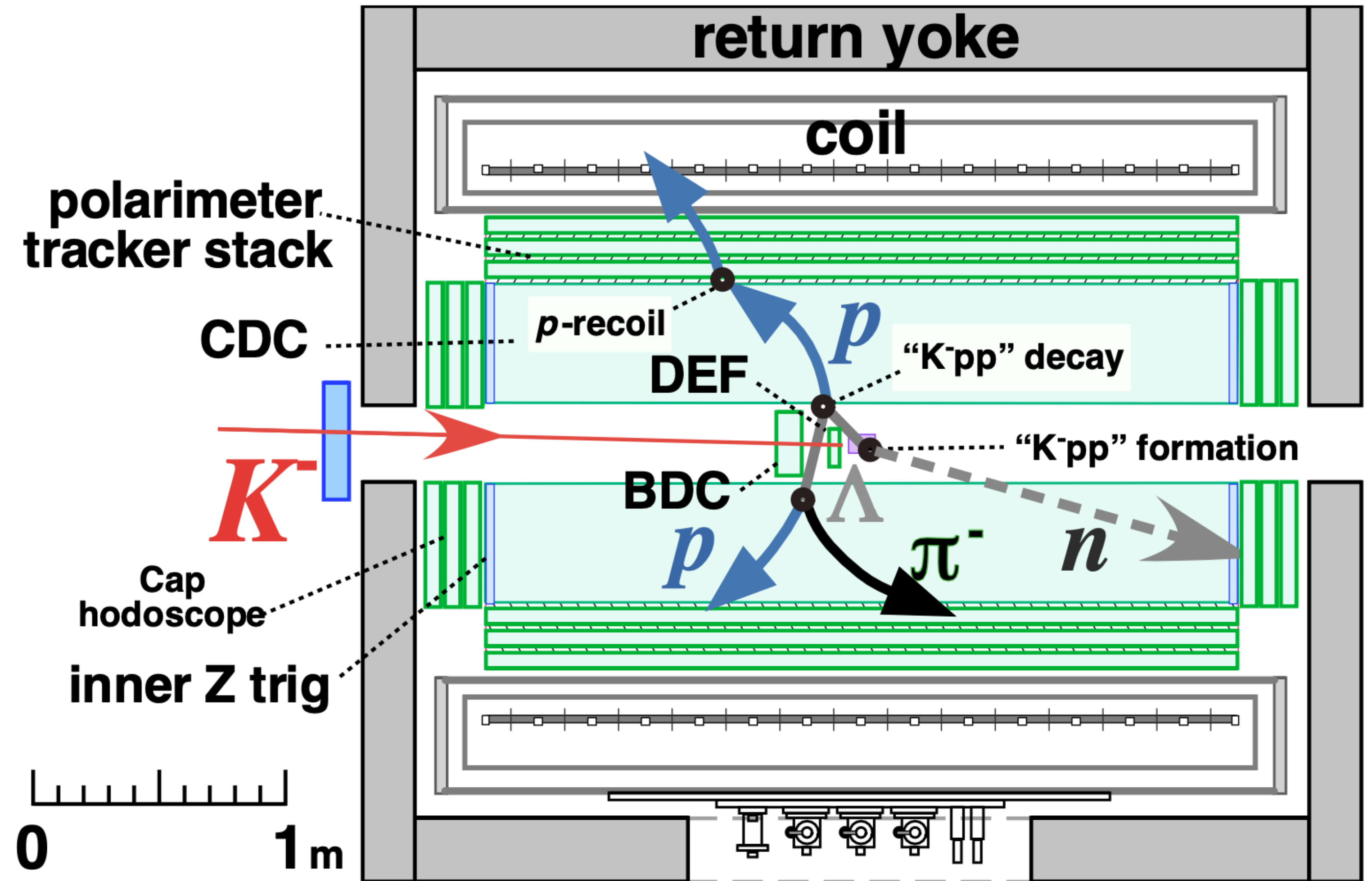


Figure 5: Schematic drawing of the CDS with a typical event.

5. Yield estimation of \bar{K}^0_{nn} production

$$\sigma_{I_{\bar{K}NN}^{(z)}}^{JP} = R_{\bar{K}NN} \times \sum_{\bar{K}N} \left(\sigma_{\bar{K}N} \times C_{I_{NN}}^2 \times C_{I_{\bar{K}NN}^{(z)}}^2 \times \mathcal{A}_N \right), \quad (3)$$

where $R_{\bar{K}NN}$ is the $\bar{K}NN$ formation probability, $\sigma_{\bar{K}N}$ ($\bar{K}N = K^-p \rightarrow K^-p$, $K^-p \rightarrow \bar{K}^0n$, and $K^-n \rightarrow K^-n$) is the elementary cross section at $\theta_N = 0$, $C_{I_{NN}}$ and $C_{I_{\bar{K}NN}^{(z)}}$ are Clebsch-Gordan coefficients for isospin coupling of NN ($I_{NN} = 1, 0$) and $\bar{K}NN$ ($I_{\bar{K}NN}^{(z)} = \pm 1/2$) systems, respectively, and \mathcal{A}_N is effective proton or neutron number of ${}^3\text{He}$.

- Effective proton numberとは？

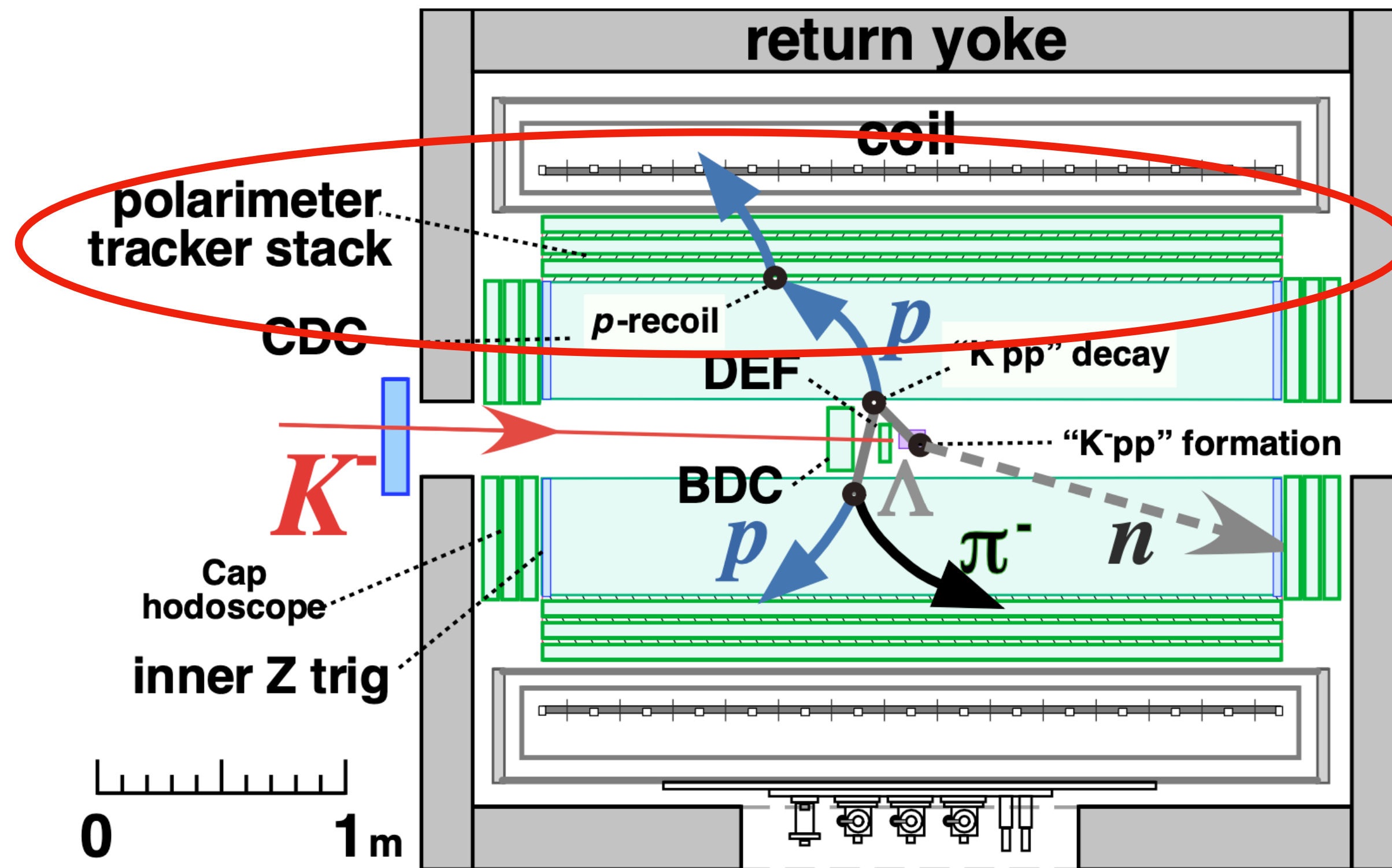
$$\text{今の場合、 } 2^{2/3} < A_p < 2 \quad A_n = 1$$

- Isospin symmetryより formation probability R は等しいと仮定

9/7~

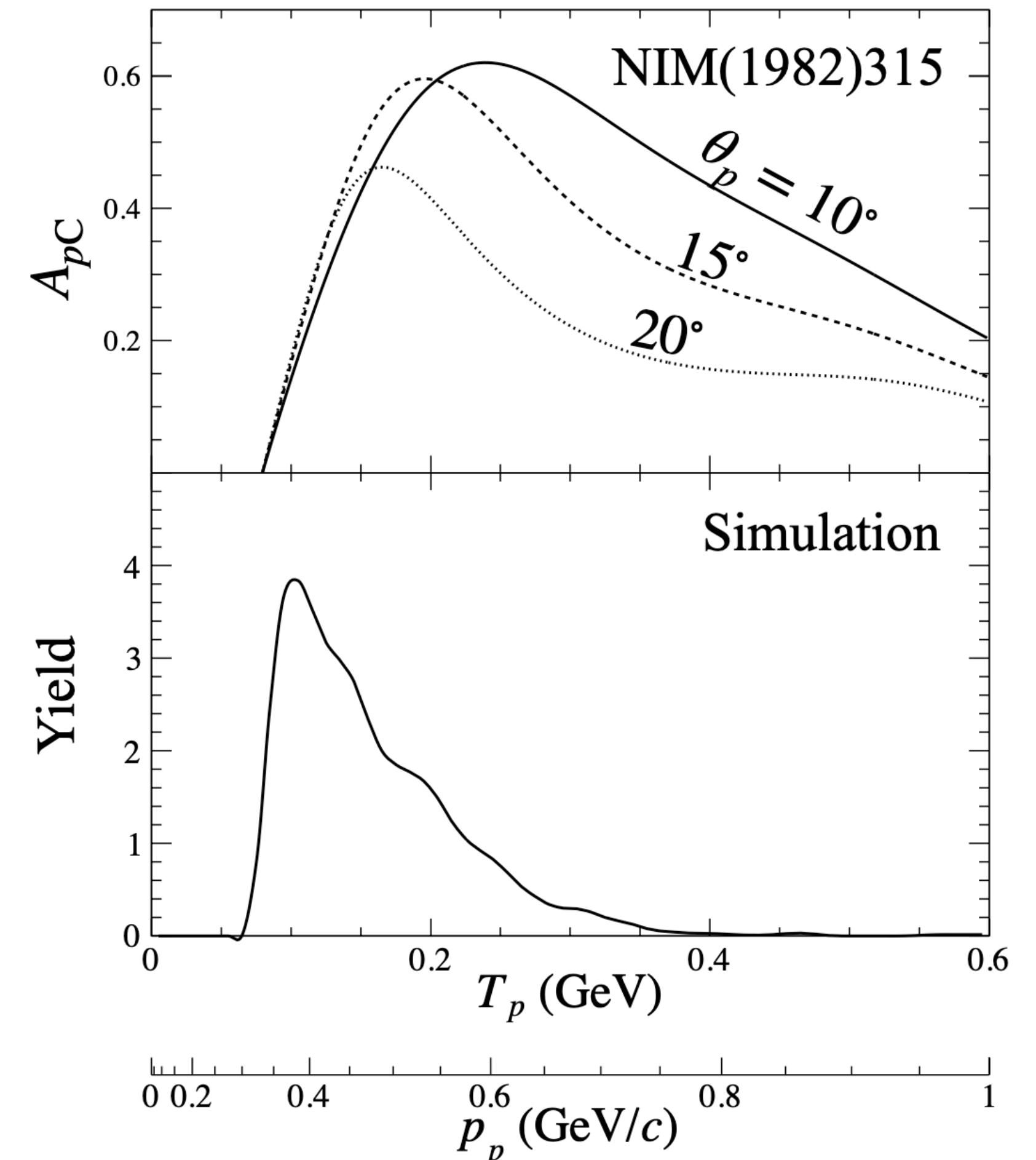
6. Sensitivity of expected Λp asymmetry on $\phi_{\Lambda p}$

- spin-spin相関 $\alpha_{\Lambda p}$ の測定で J^P を決定できる。
- Λ のCM系ではそのスピン方向に p が出やすい。 $\rightarrow \Lambda$ のスピン決定
- $K^-pp \rightarrow \Lambda p$ で出てくる p のスピン測定 \rightarrow asymmetric nuclear scattering



- 平均analyzing power $\langle A_{pC} \rangle \sim 0.3$

θ_p : scattering angle



6. Sensitivity of expected Λp asymmetry on $\phi_{\Lambda p}$

- いくつかの考慮ポイント

Nuclear scattering asymmetryは粒子の運動量方向に対する、スピンの垂直成分に対して現れる。

結局は全角運動量保存

CDS内の磁場によるCyclotron motionとスピンのLarmor precession

$K^-pp \rightarrow \Lambda p$ の崩壊軸と $S_{\Lambda p}$ は直交する。(なぜなら $L_{\Lambda p} \perp S_{\Lambda p}$) ?

- $J^P = 0^-$ の場合、

the situation is bit more complicated. The 1/3 of $\bar{K}NN$ decay to $S_{\Lambda p} = 0$ ($\alpha_{\Lambda p} = -1$), thus this component is spherical. The other 2/3 component decay to $S_{\Lambda p} = 1$ ($\alpha_{\Lambda p} = +1$), so the angular momentum $L_{\Lambda p} = 1$ must be orthogonal to the spin $S_{\Lambda p} = 1$ to be $J = 1$, thus the spin is \sim parallel to the “ K^-pp ” decay axis (see Appendix B in detail).

6. Sensitivity of expected Λp asymmetry on $\phi_{\Lambda p}$

Lab系

$\theta_{\vec{S}_p - \vec{v}_p}$: proton spinとmotional axisのなす角

$\theta_{\vec{S}_p - \vec{v}_p}$ を得られれば J^P は容易にわかるが、
残念ながら実験的に不可能。

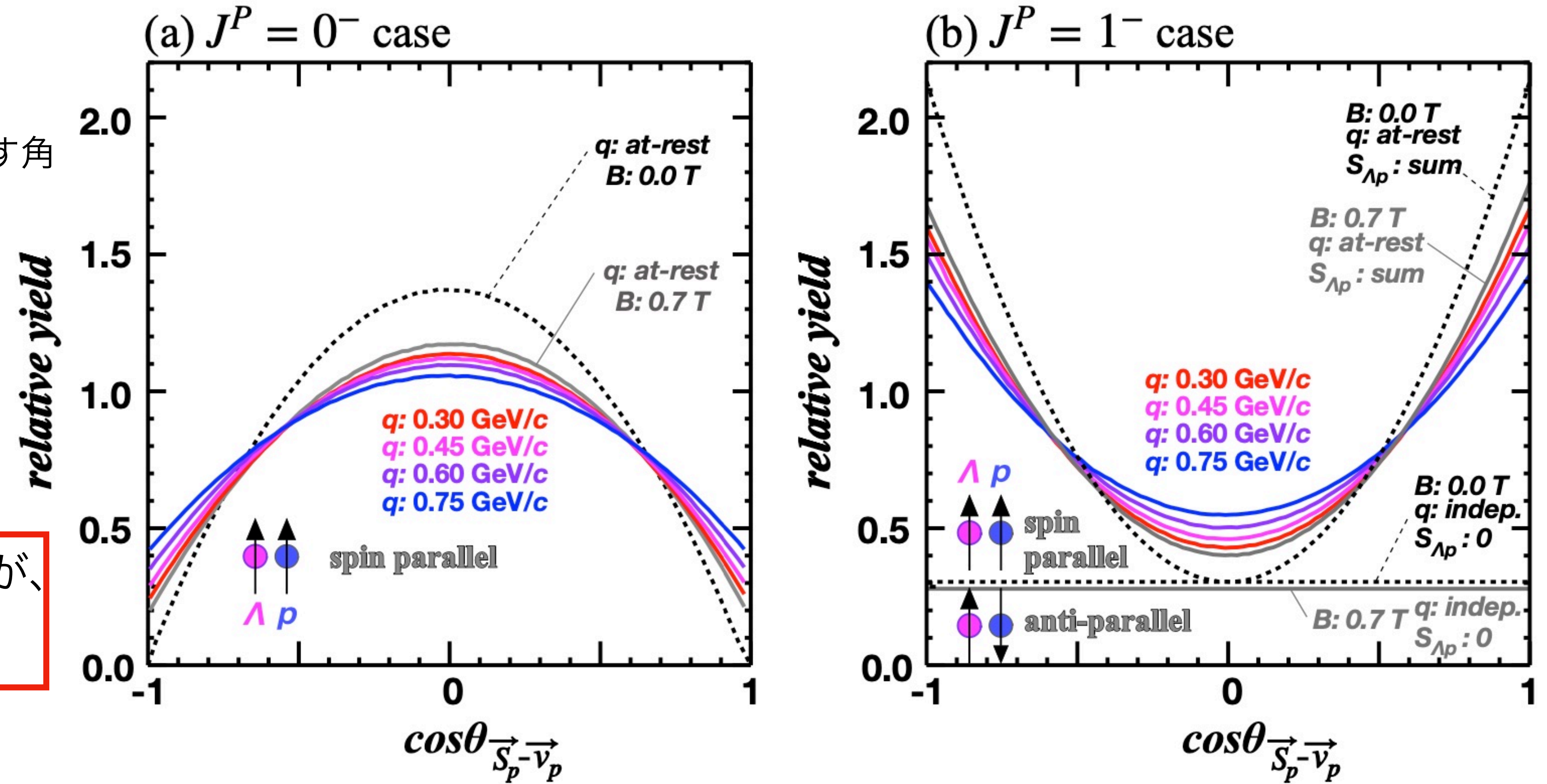


Figure 7: $\cos \theta_{\vec{S}_p - \vec{v}_p}$ distribution for (a) $J^P = 0^-$ and (b) $J^P = 1^-$. The black dotted lines show distribution without magnetic field nor boost of K^-pp . The colored lines show distribution including both magnetic field and boost effects.

6. Sensitivity of expected Λp asymmetry on $\phi_{\Lambda p}$

測定できるのは Λ と p のspin-spin相関である。

P16の最後の段落から何言ってるかわからなくなりました、、、

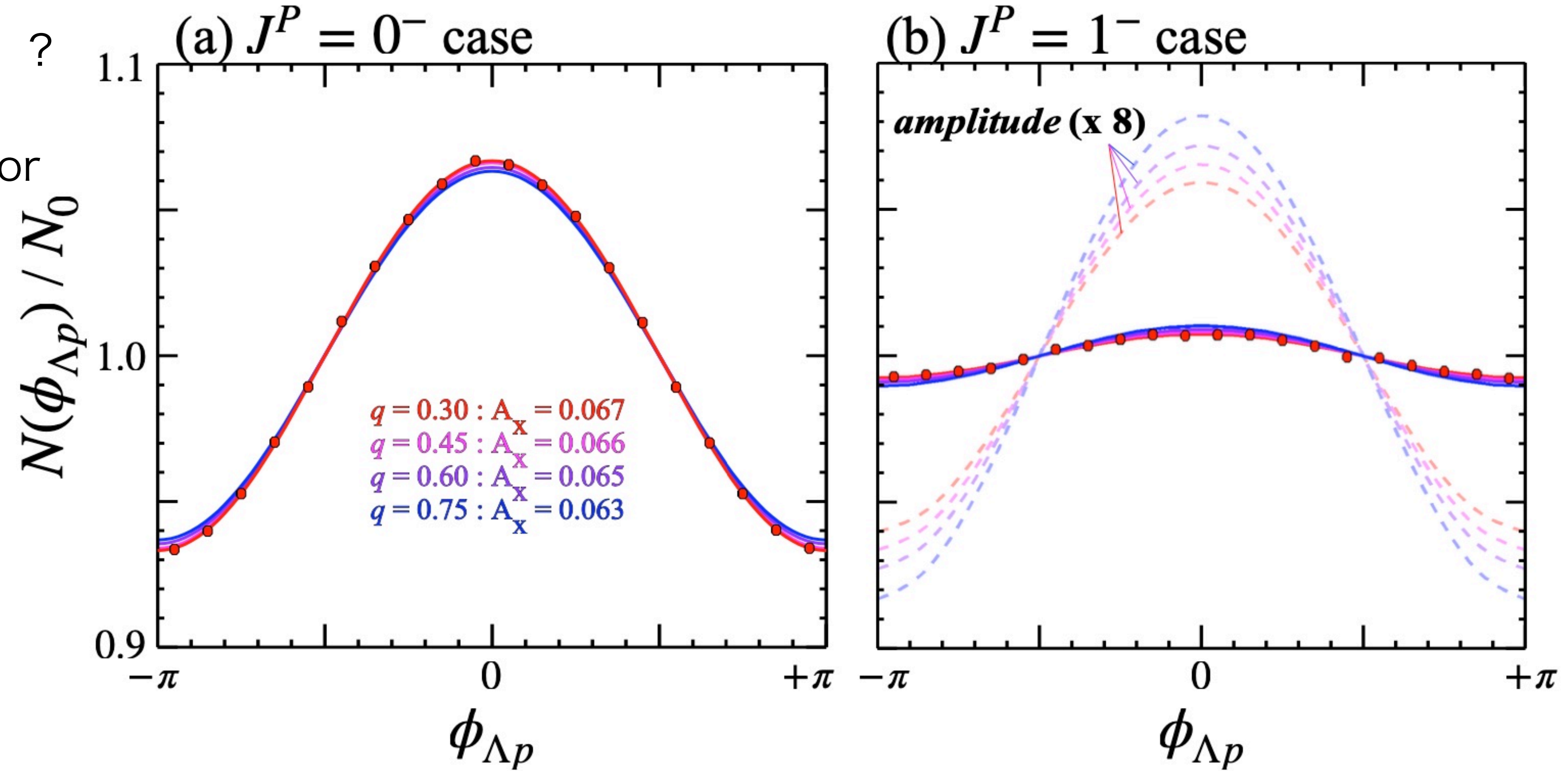
6. Sensitivity of expected Λp asymmetry on $\phi_{\Lambda p}$

$\phi_{\Lambda p}$ 分布の非対称性は $\alpha_{\Lambda p}$ より小さい。 ?

r^{J^P} : the correlation reduction factor

およそ $r^{J^P} \sim 0.065$ for $J^P = 0^-$

$r^{J^P} \sim 0.010$ for $J^P = 1^-$



Note that ~以下?

Figure 8: $\phi_{\Lambda p}$ distribution for (a) $J^P = 0^-$ and (b) $J^P = 1^-$. The vertical axes are scaled by $N_{bin} / \int N(\phi_{\Lambda p})$, so as to make the distribution $1 + r^{J^P} \alpha_{\Lambda p} \cos \phi_{\Lambda p}$.

7. Detection of isospin doublet, ' $\bar{K}^0 nn$ ', and isospin symmetry study by the mass determination

4つの終状態が考えられる

- “ $\bar{K}^0 nn$ ” production (decay into Λn), $\sigma_{\bar{K}^0 nn} \cdot \text{BR}_{\Lambda n} = 1.2 \sim 1.4 \mu\text{b}$ ($J^P = 0^-$ assumption)
- quasi-free reaction going to Λn channel ($\text{QF}_{\Lambda n}$), $\sigma_{\text{QF}_{\Lambda n}} = 3.6 \sim 4.1 \mu\text{b}$
- “ $K^- pp$ ” production (decay into Λp), $\sigma_{K^- pp} \cdot \text{BR}_{\Lambda p} = 9.3 \mu\text{b}$
- quasi-free reaction going to Λp channel ($\text{QF}_{\Lambda p}$), $\sigma_{\text{QF}_{\Lambda p}} = 10.7 \mu\text{b}$

E15で得られた

・ 拡大したacceptanceのおかげで、' $\bar{K}^0 nn$ 'も測定可能に。 Λp を測定して、missing neutronで終状態 Λpn が上のどれかなのかを特定できる。

・ 直接 Λn を検出するよりも Λp を検出してmissing neutron windowを課した方が収率が高い。

7. Detection of isospin doublet, ‘ $\bar{K}^0 nn$ ’, and isospin symmetry study by the mass determination

High momentum transfer regionをカットすることでみたいものがはっきり出てくる。

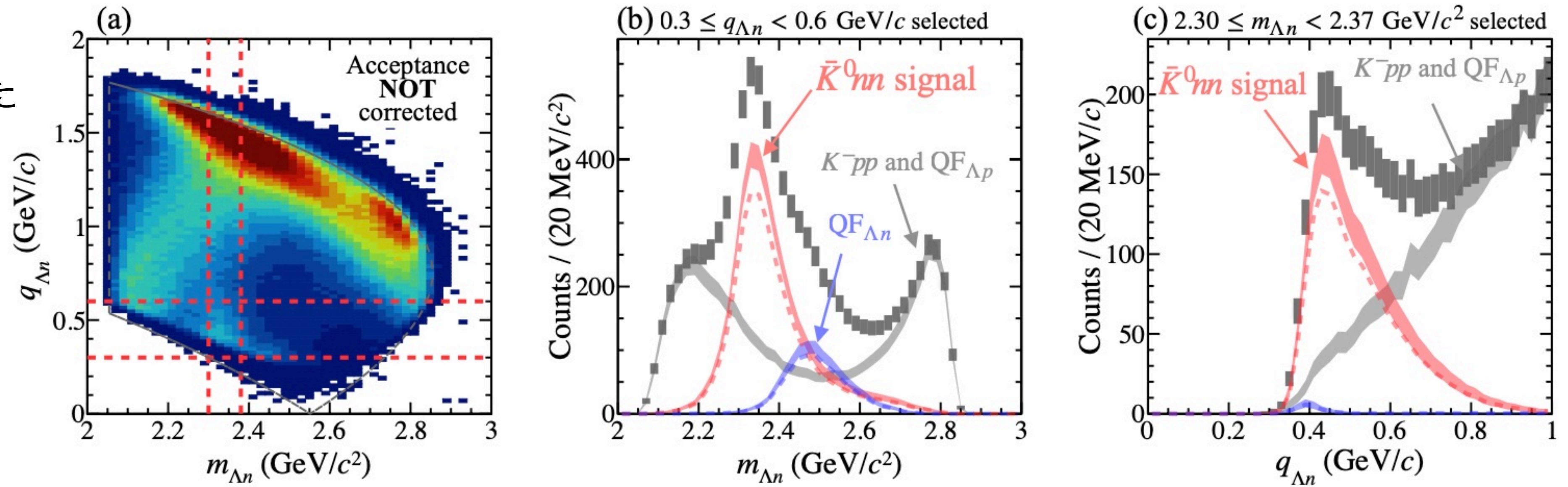


Figure 9: Expected result for the “ $\bar{K}^0 nn$ ” measurement, assuming J^P of “ $K^- pp$ ” observed in E15 to be 0^- . (a) two-dimensional distribution on the invariant-mass of Λn ($m_{\Lambda n}$) and momentum transfer to Λn ($q_{\Lambda n}$). (b) Projection spectrum on the $m_{\Lambda n}$ axis by selecting $0.3 \leq q_{\Lambda n} < 0.6$ GeV/c region. (c) Projection spectrum on the $q_{\Lambda n}$ axis by selecting $2.3 \leq m_{\Lambda n} < 2.37$ GeV/c region. The dotted histograms in the projections show the case of the expected yield to be minimum with smaller effective proton number $\mathcal{A} = 2^{2/3}$.

7. Detection of isospin doublet, ' \bar{K}^0_{nn} ', and isospin symmetry study by the mass determination

$J^P = 1^-$ だったら検出は簡単

P22 [The present~]のところ、
compared to Λp modeと書いてい
ますが、 Λn modeの間違いでは？

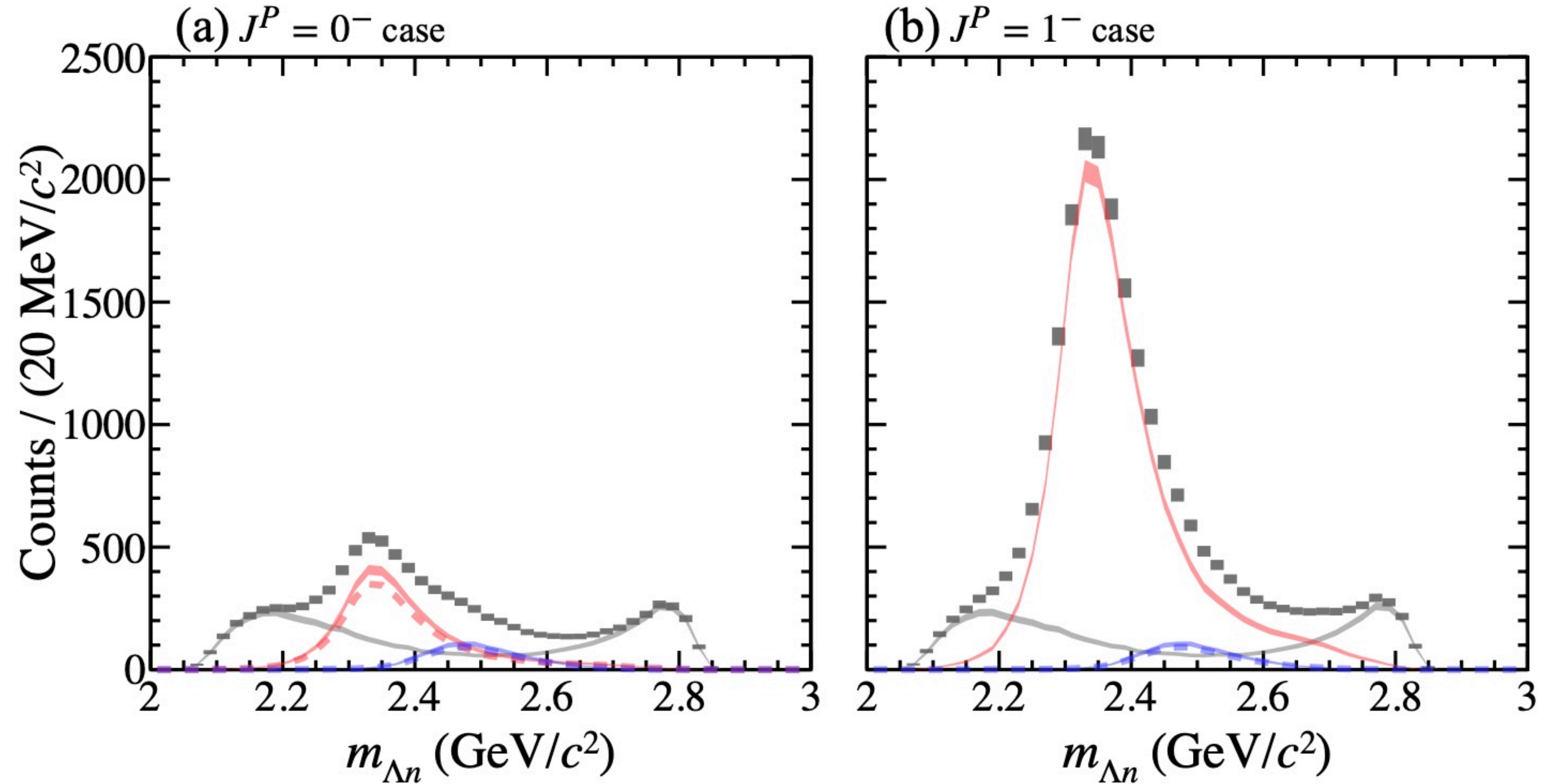


Figure 10: Expected invariant-mass spectra of Λn -pair by selecting $0.3 \leq q_{\Lambda n} < 0.6$ GeV/c region for (a) $J^P = 0^-$ (same as Fig. 9-(b)) and (b) $J^P = 1^-$. In the case of $J^P = 0^-$, expected yield slightly changed if $\mathcal{A} = 2^{2/3}$ as shown by dotted histograms.

7. Detection of isospin doublet, ' \bar{K}^0_{nn} ', and isospin symmetry study by the mass determination

- ・ Λn modeの解析も重要。 q のカットオフ($\sim 0.4\text{GeV}/c$)は物理から来ているのではなく、CDSのアクセプタンスから来ている。
- ・ 本来は、運動学的に許される全領域の観測が、reaction mechanism and dynamics of the $\bar{K}NN$ bound stateのクリアな理解には不可欠。

8. Measurement of α_{Λ}

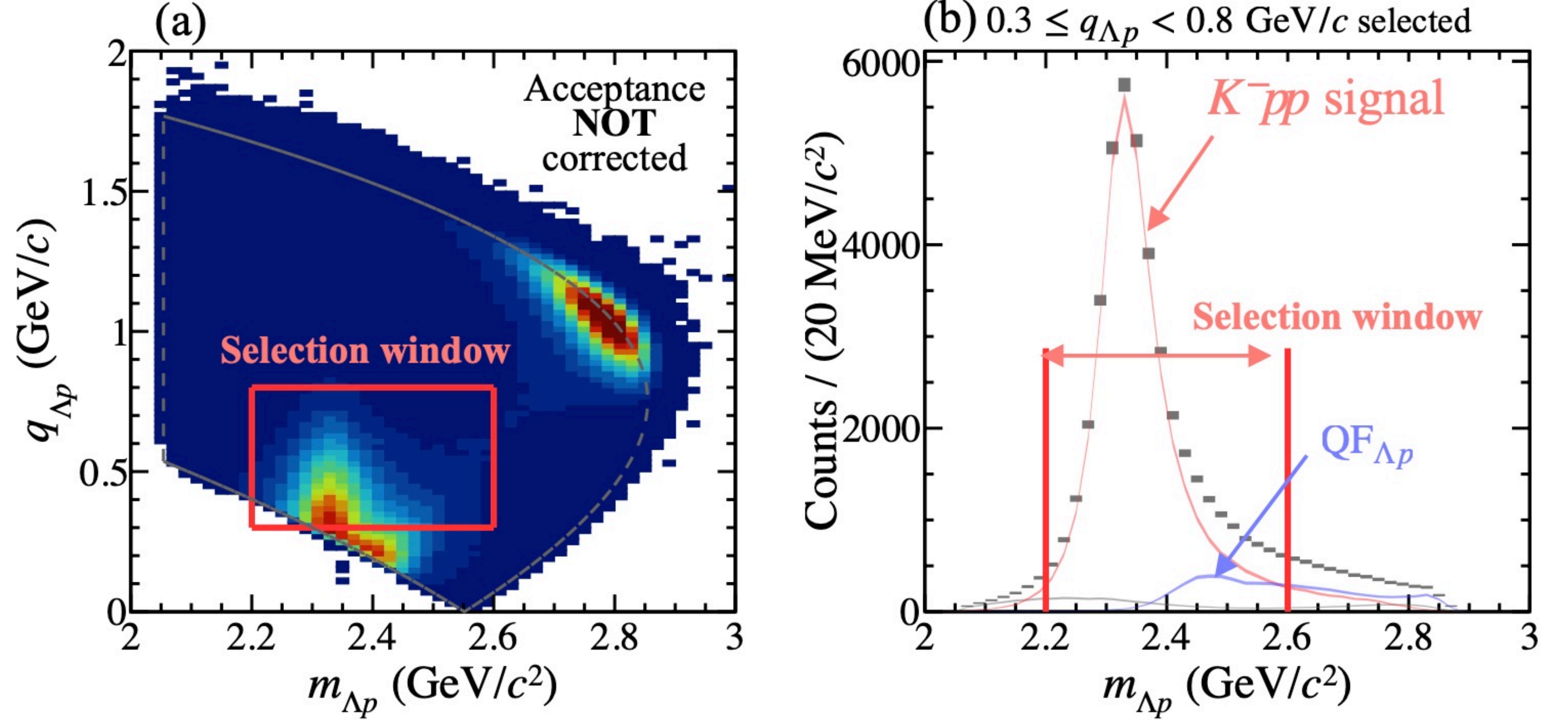


Figure 11: Expected spectra of “ K^-pp ” measurement. (a) two-dimensional distribution on the invariant-mass of Λp ($m_{\Lambda p}$) and momentum transfer to Λp ($q_{\Lambda p}$). (b) Projection spectrum on the $m_{\Lambda p}$ axis by selecting $0.3 \leq q_{\Lambda p} < 0.8 \text{ GeV}/c$ region. The red box in (a) and red lines in (b) are selection window for $\alpha_{\Lambda p}$ measurement.

8. Measurement of $\alpha_{\Lambda p}$

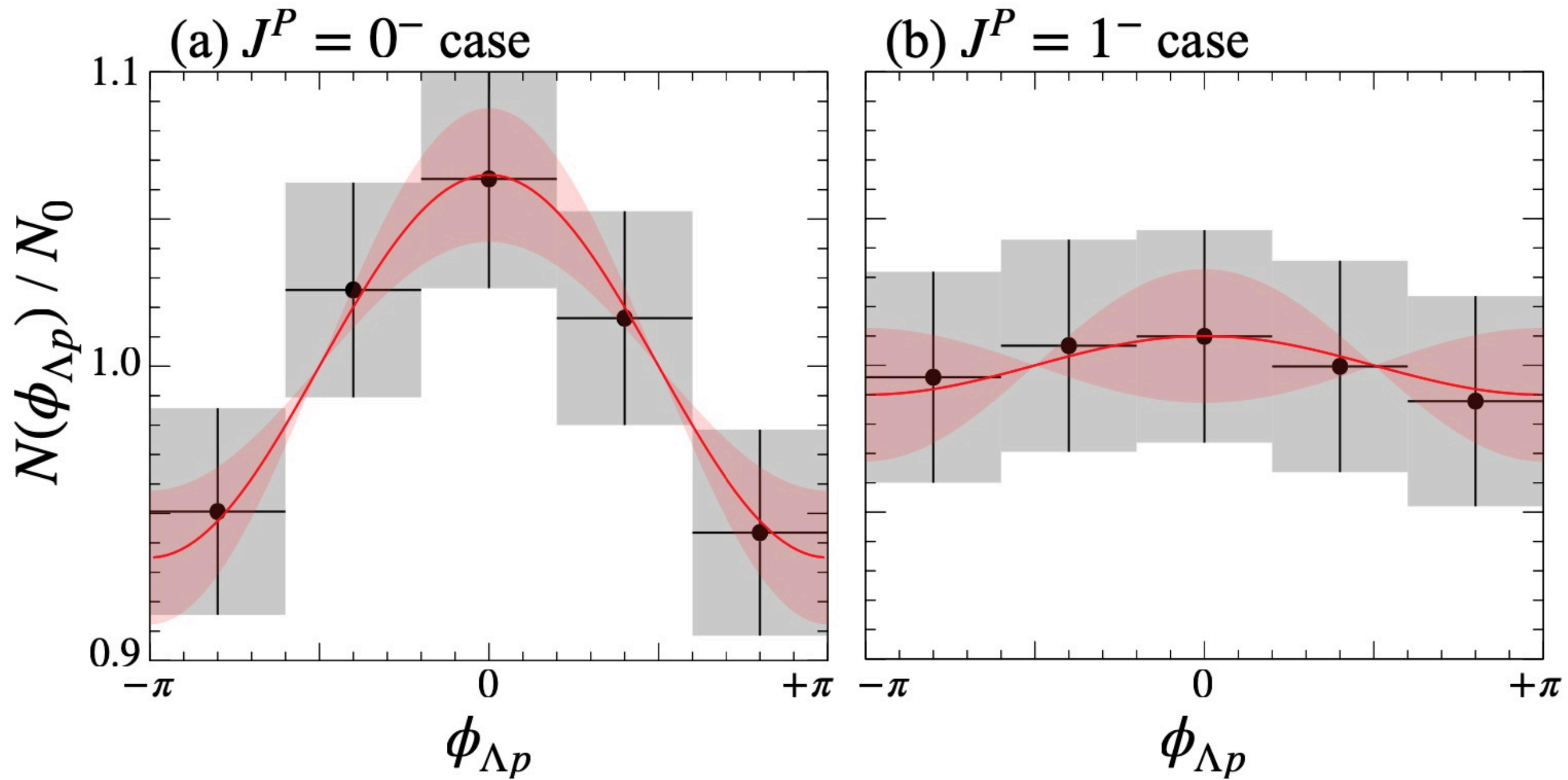
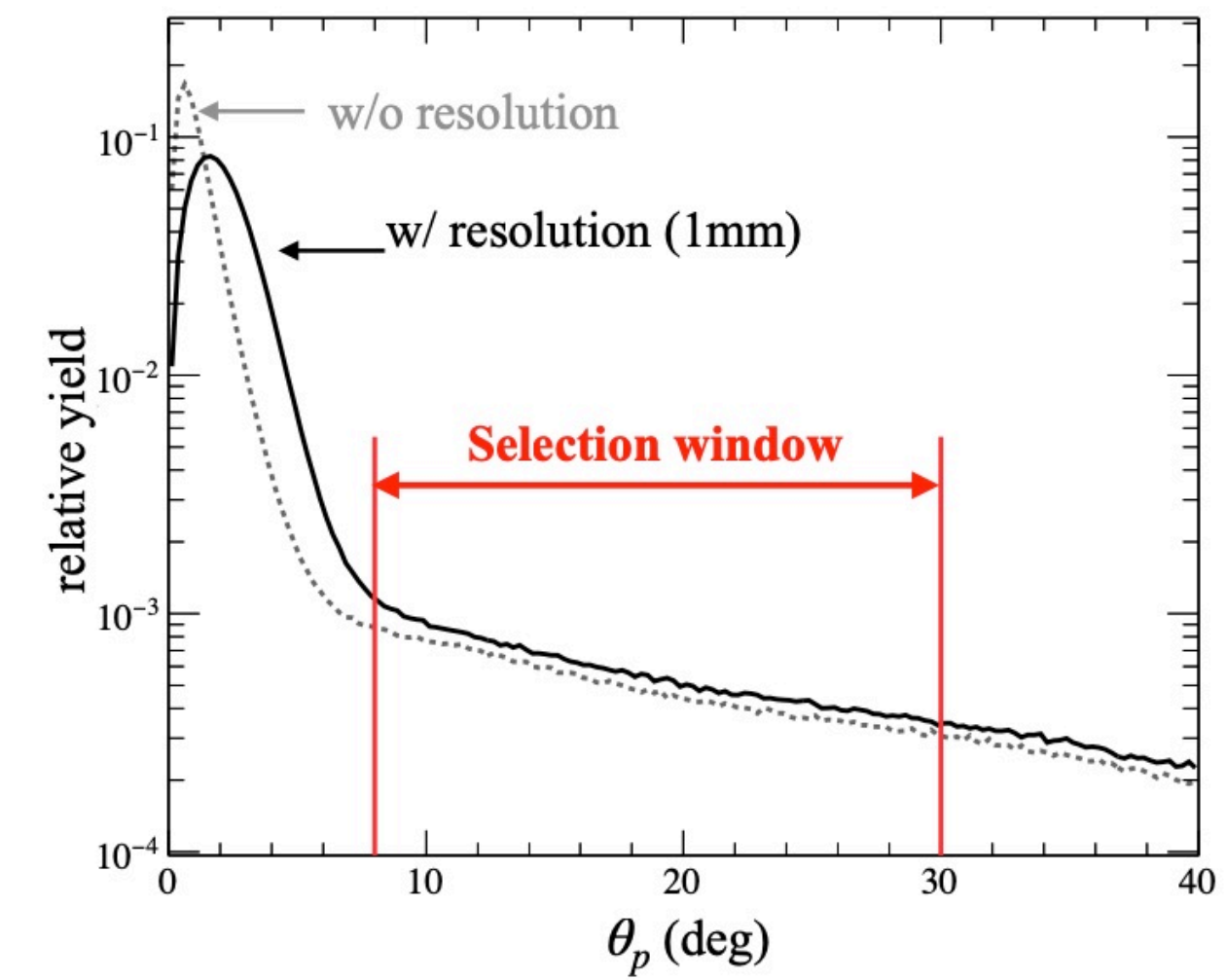


Figure 13: Expected $\phi_{\Lambda p}$ -distribution for “ $K^- pp$ ” $\rightarrow \Lambda p$ decay with 8 weeks beam-time for (a) $J^P = 0^-$ and (b) $J^P = 1^-$. The red line and red band shows fitting result and 1σ region.



ed θ_p -distribution with (black) and without (gray dotted) detector or tracker in the polarimeter). Spin sensitivity in the multiple scattering region (very forward region) is quite weak, so we set the selection window by the red lines.

9. Summary of objectives